Multiplicity among solar–type stars. III. Statistical properties of the F7-K binaries with periods up to 10 years

J. L Halbwachs, M. Mayor, S. Udry, Frédéric Arenou

A&A 397, 159–175 (2003)
DOI: 10.1051/0004-6361:20021507

Astronomy & Astrophysics

Multiplicity among solar–type stars

III. Statistical properties of the F7–K binaries with periods up to 10 years⋆

J. L. Halbwachs[1], M. Mayor[2], S. Udry[2], and F. Arenou[3]

[1] Observatoire Astronomique de Strasbourg (UMR 7550), Observatoire Astronomique, 11 rue de l'Université, 67 000 Strasbourg, France
[2] Geneva Observatory, 51 chemin des Maillettes, 1290 Sauverny, Switzerland
e-mail: Michel.Mayor@obs.unige.ch;Stephane.Udry@obs.unige.ch
[3] Observatoire de Paris–Meudon, bât. 11, 5 place J. Janssen, 92195 Meudon Cedex, France
e-mail: Frederic.Arenou@obspm.fr

Received 4 July 2002 / Accepted 1 October 2002

Abstract. Two CORAVEL radial velocity surveys – one among stars in the solar neighbourhood, the other in the Pleiades and in Praesepe – are merged to derive the statistical properties of main–sequence binaries with spectral types F7 to K and with periods up to 10 years. A sample of 89 spectroscopic orbits was finally obtained. Among them, 52 relate to a free–of–bias selection of 405 stars (240 field stars and 165 cluster stars). The statistics corrected for selection effects yield the following results: (1) No discrepancy is found between the binaries among field stars and the binaries in open cluster. The distributions of mass ratios, of periods, the period–eccentricity diagram and the binary frequencies are all within the same error intervals. (2) The distribution of mass ratios presents two maxima: a broad peak from $q \approx 0.2$ to $q \approx 0.7$, and a sharp peak for $q > 0.8$ (twins). Both are present among the early–type as well as among the late–type part of the sample, indicating a scale–free formation process. The peak for $q > 0.8$ gradually decreases when long–period binaries are considered. Whatever their periods, the twins have eccentricities significantly lower than the other binaries, confirming a difference in the formation processes. Twins could be generated by in situ formation followed by accretion from a gaseous envelope, whereas binaries with intermediate mass ratios could be formed at wide separations, but they are made closer by migration led by interactions with a circumbinary disk. (3) The frequency of binaries with $P < 10$ years is about 14%. (4) About 0.3% of binaries are expected to appear as false positives in a planet search. Therefore, the frequency of planetary systems among stars is presently 7^{+4}_{-2}%. The extension of the distribution of mass ratios in the planetary range would result in a very sharp and very high peak, well separated from the binary stars with low mass ratios.

Key words. stars: binaries: general – stars: binaries: spectroscopic – stars: formation – stars: low–mass, brown dwarfs

1. Introduction

The distributions of fundamental parameters of binary stars have been searched for and debated over for three quarters of century (since Öpik 1924), but we still did not have a definitive answer. This controversy comes essentially from its importance for our understanding of star formation. It is well–known that the majority of stars belong to double or multiple systems, and any realistic model of star formation must allow the generation of binary stars having the statistical properties which are observed. This interest increased after the discovery of the extrasolar planets, when it was suggested that these new objects could have the same origin as double stars (Stepinski & Black 2000).

Send offprint requests to: J. L. Halbwachs,
e-mail: halbwachs@astro.u-strasbg.fr

⋆ Based on photoelectric radial–velocity measurements collected at Haute-Provence observatory and on observations made with the ESA Hipparcos astrometry satellite.

1.1. Binary formation

The formation process of binary stars is still poorly understood, and various mechanisms could intervene (see the recent IAU symposium 200, and the conclusion by Mathieu 2001). Whatever the model, the complete formation process consists of two phases: the fragmentation producing condensing cores which will become the components of the binary, and the later evolution, consisting in accretion and migration, which will fix the final masses of the components and the orbital parameters of the systems.

1.1.1. Fragmentation

Fragmentation may occur at three different phases of the condensation of a molecular cloud (see the reviews by Bonnell 2001a,b). The earliest one is the first phase of the gravitational collapse. The cloud is split in several condensing fragments, with centers separated by thousands of AU.

The first phase of the condensation ends when the gas is no longer optically thin. The gravitational collapse is then stopped, and the temperature grows, impeding fragmentation.

A second collapse begins when the core is hot enough to induce the dissociation of the molecular hydrogen. Fragmentation during or after the second collapse could generate a *seed* binary with components as close as 0.1 AU. However, this process requires very specific conditions, and it is unlikely to happen in reality. Another process leading to close condensing cores is the formation of a disk around the protostar, and its fragmentation (Bonnell & Bate 1994). Whatever the process, the masses of the two cores are roughly proportional to the separation (Bate 2000): when the separation is about 0.1 AU, the component mass is only about 0.005 $\mathcal{M}_\odot$.

1.1.2. Evolution

The continuation of binary formation, from condensing cores to the final binary, could follow three different scenarios.

The evolution of a cluster of protostars is led by dynamical interactions (see Bodenheimer & Burkert 2001; Clarke 2001). Some binaries or multiple systems may be formed when the cluster is disrupted. Although the tail of the distribution may contain close binaries, separations below 10 AU are expected to be rather rare. The orbits of these systems should be eccentric. The final mass ratios depend on dynamical exchange interactions: the encounter of a binary with a single star heavier than the secondary component typically results in the ejection of the secondary and the capture of the originally single star. The distribution of masses of the components depends on the number of cores generated by fragmentation. When it is larger than 2, the distribution of secondary masses does not depend on the primary mass. In other words, the distribution of mass ratios varies with the mass of the primary components.

When a circumbinary disk is formed, the transfer of angular momentum from the binary to the disk results in a decrease of the semi–major axis and an increase of the eccentricity (Artymowicz et al. 1991). If material is transferred from the disk to the binary, the mass ratio may increase (Artymowicz & Lubow 1994; Günther & Kley 2002) or decrease (Günther & Kley 2002). Close binaries could thus result from migration of wide pairs, but the investigations into this process are not advanced enough to evaluate whether it is sufficiently efficient to explain the frequency of close binaries (Artymowicz & Lubow 2001).

When a close seed binary is formed in situ, the components have low initial masses and they still receive a large part of their final mass. The result of accretion from a gaseous envelope depends on the specific angular momentum of the infalling matter (see the review by Bate 2001): when it is low, the semi–major axis and the mass ratio both decrease. A high specific angular momentum does the opposite: the separation between the components increases, and the mass ratio grows until unity. The evolution of eccentricity was somewhat neglected in recent investigations. However, Artymowicz (1983) concluded that the eccentricity is usually decreasing, especially for large mass ratios. Bate (2000) also found that, unlike migration led by a disk, it seems that accretion generates low eccentricities.

In a very recent paper, Bate et al. (2002b) simulated the formation of binary stars in a small cluster as a hydrodynamical process, taking all these effects into account. They concluded that equal–mass systems should be frequent among close binaries, and that the frequency of close binaries should increase with the mass of the primary. They predicted also that close binaries should often have wide companions.

1.1.3. Minimum secondary mass

It follows from the above that the final mass ratio of a binary is the product of two consecutive processes: fragmentation and accretion. Since a large amount of material is accreted, Bate et al. (2002a) estimate that the final mass of any component should usually be above the hydrogen–burning limit. Brown dwarfs are then *failed* stars which were ejected from dynamically unstable systems, and they are expected to be rare among binary components.

1.2. History of binary statistic

It results from the previous section that the distributions of mass ratios, of periods and of eccentricities of main sequence binaries are important observational clues for validating the models. However, these distributions are difficult to derive in practice: the statistics of binary samples are biased by selection effects, and the relevant physical parameters are sometimes not directly observed. Therefore, the results of the investigations look curiously unstable and varying. This concerns not only distributions derived from different classes of binaries, such as visual binaries or spectroscopic binaries, but also results obtained by different studies related to the same kind of objects. About this aspect, the most critical parameter is the mass ratio, hereafter defined as the ratio of the masses, $q = \mathcal{M}_2/\mathcal{M}_1$.

1.2.1. Mass ratios

When only spectroscopic binaries are considered, the distributions of mass ratios that were derived may be distributed in two categories :

– *The double–peak distributions*. This distribution was often found in studies based on all known spectroscopic binaries (Trimble 1974, 1978; Staniucha 1979). It consists of one peak of equal–mass components, and one peak around $q \approx 0.2$ or 0.3. The former corresponds to the double–lined spectroscopic binaries (SB2), and the latter to the single–lined binaries (SB1). Tout (1991) generated a similar double–peak distribution by randomly picking stars obeying the initial mass function but within restricted ranges of masses. The peak around $q = 1$ was also obtained and commented in studies devoted to the SB2 alone (Lucy & Ricco 1979; Tokovinin 2000).
However, binaries with equal–mass components are brighter than binaries with light and therefore faint secondary components, and their frequency may be increased

by a selection based on apparent magnitude. This peak disappears when it is assumed that the sample of known SB is fully affected by this bias (Halbwachs 1987). The rising frequency for small q is doubtful, on one hand since SB with small q are difficult to detect, and on the other hand because it was usually obtained by computing approximately the mass ratio of each SB1, assuming they have all the same orbital inclination. This method is inadequate for calculation of the statistics, since it systematically generates a peak in the frequency of small mass ratios (see the simulations by Halbwachs 1981, and by Mazeh & Goldberg 1992). Nevertheless, the bimodal distribution was sometimes also derived from the photometric study of binaries in open clusters (Kähler 1999); the artifact of the treatment of SB1 and the bias toward large mass ratios cannot be then invoked, but other factors may intervene, such as a contamination by triple systems.

– *The monotonic distributions*. In order to properly take into account the selection effects, the properties of binaries were also derived from SB found in the course of binary surveys among exhaustive samples clearly defined. The first approach was the survey of Abt & Levy (1976). They used a new method of calculation of the distribution of q, and they found a distribution increasing from the small mass ratios until $q = 1$. However, this result was critiqued since they neglected the effect of a selection based on apparent magnitude (Branch 1976), and also because several SB in their sample were spurious (Morbey & Griffin 1987). Another study was performed among F7–G dwarfs in Paper II of the present series (Duquennoy & Mayor 1991). In order to avoid the bias coming from a selection based on magnitudes, they analysed the SB detected in sample of nearby stars with known parallaxes (Paper I: Duquennoy et al. 1991). Their results were improved with the inversion algorithm of Mazeh & Goldberg (Mazeh et al. 1992), and a distribution slightly increasing was finally obtained. However, due to the small number of SB in their sample, the errors are rather large, and a flat or a decreasing function would still be compatible with their data. In fact, the SB surveys provide monotonic distributions of mass ratios simply because they involve too few stars to reveal complex features. However, details appear, but with a low significance: when the SB sample in Paper II was analysed again by Heacox (1995, 1998), he found a well–marked peak for $q = 0.2$, and possibly a second one for $q > 0.8$. He estimated that the low frequency of SB with $q < 0.2$ could be due to a selection effect, and that the distribution could be decreasing from $q = 0$ to $q = 0.8$ or even $q = 1$.

Alternatively, it was proposed that the closest binaries could have preferably equal–mass components, but that the long period systems usually have components with quite unequal masses. This idea was supported by Abt & Levy (1976), who estimated that the transition period separating the two regimes is around 10 or 100 years – in practice, this corresponds to the transition between SB and VB in their sample. A new argument in that sense arises from the statistics of the close visual binaries observed by Hipparcos: Söderhjelm (1997) found that the frequency of equal magnitude binaries gradually decreases when the separation increases. However, it was also suggested that this transition could be well within the SB range of period: it is only 25 days for Lucy & Ricco (1979), and 40 days for Tokovinin (2000). Unfortunately, these results were obtained from all SB2 with published orbits, and it cannot be excluded that the difference between short and long period systems comes from the various selection effects which intervene on a so non–homogeneous sample. The most obvious is the difficulty to separate the lines of equal components on a blended spectrum when the RV amplitude is small. The binary is then detected, but the derivation of the orbit requires much more effort than when the lines are well separated. This bias could explain why the twins are more frequent among short period binaries, which usually have large RV amplitude. It was also investigated whether the frequency of equal–mass components was larger among the closest binaries in the Paper II sample but only a slight (i.e. poorly significant) correlation was found (Heacox 1998).

1.2.2. Periods

The distribution of the periods of a sample of binary stars reflects the technique used to build up the sample. The periods of the SB range from a few hours to a few years, the visual binaries range from a few years to a few centuries, and the common proper motion pairs from a few centuries to million years, if they are really orbiting. Therefore, the derivation of the overall distribution is very sensitive to the corrections of the selection effects. The most frequent result is a bell–shaped distribution of $\log P$, with a maximum in the visual binary range (around $P = 180$ years in Paper II).

1.2.3. Eccentricities

The eccentricities are correlated with the periods (Paper II). Binaries with periods shorter than about 10 days usually have a circular orbit, due to tidal interactions between the components. For long period binaries, the eccentricity ranges from about 0.1 to near 1. A striking feature of the (e – $\log P$) distribution is the lack of any circular orbit for periods larger than about 10 days. A correlation between the eccentricities and the secondary masses was investigated in Paper II, but no convincing result was obtained.

1.3. Paper organization

The present paper is a revision and a continuation of the investigations initiated in Paper II of spectroscopic binaries. The results of the SB survey among K-type nearby stars (Udry et al. 2002, Paper IV hereafter) are added to the sample of F7–K dwarfs, and the definition of the sample in Paper II is entirely revised on the basis of the Hipparcos parallaxes. The calculation of the distribution of the mass ratios is also different, and it makes use of the constraints coming from the astrometric orbits derived in Paper IV. Moreover, SB found in open clusters are added to our sample, in order to get enough objects

to derive significant features in the distribution of mass ratios. Correlations were searched for between the mass ratios and various parameters, namely the periods, the spectral types, the eccentricities and the sample origins of the stars.

The selection of the sample of solar neighbourhood stars is discussed in Sect. 2. The search in the open clusters, published a few years ago, is summarized in Sect. 3. The samples are compared and merged in Sect. 4. The selection effects are investigated in Sect. 5. The statistical properties of the binaries are derived in Sect. 6 and are presented in Sect. 7. The implications on binary formation are discussed in Sect. 8.

2. The samples of dwarf stars in the solar neighbourhood

The main characteristics of the SB survey in the solar neighbourhood are presented in Paper IV. We obtained the radial velocities of more than 600 stars with spectral types F, G or K observable from Haute-Provence. The stars were taken from the catalogue of Nearby Stars (Gliese 1969, CNS hereafter), from its supplement (Gliese & Jahreiss 1979), and from the preliminary version of the third edition of the CNS (Gliese & Jahreiss 1991). They were observed several times during about 9 years, and more than 80 SB orbits were derived. Our purpose is now to derive the statistical properties of binaries with unevolved components. This cannot be done from the entirety of the stars which were observed, essentially for two reasons: the first one is that the CNS contains some giant stars that were erroneously classified as dwarfs. The second reason is that the distribution of binaries with mass ratios larger than $q = 0.5$ may be dramatically affected by a bias toward bright magnitudes. When the CORAVEL survey was initiated, the trigonometric parallaxes were too inaccurate to investigate these questions. Fortunately, the Hipparcos programme (ESA 1997) supplied very accurate parallaxes for almost all the CNS stars. Therefore, the selection of a sample for statistical use is distance–based upon these new data.

2.1. The extended sample of MS stars

Our aim is to select the main–sequence stars of the observation programme on the basis of the absolute magnitudes and of the colour indices. For that purpose, the stars with spectral types F7 to K, declination more north than $\delta = -15°$ and trigonometric parallaxes larger than 20 mas were extracted from the Hipparcos catalogue. The absolute magnitudes of these stars were calculated, and the stars were plotted in the $(B-V, M_V)$ HR diagram. The position of the mean main sequence was derived by an iterative least square calculation, taking into account only the stars closer than 3σ from the mean MS in Fig. 1. Among the CORAVEL sample, 456 F7–K stars (including a few ones with $\delta < -15°$) lie within the area defined in this figure. These stars constitute the so–called *extended* sample, and they are all listed in Tables 1 and 2. The SB of the extended sample are presented in Sect. 2.3 hereafter. It was verified that the positions of the SBs within or outside the MS strip were not altered by the contributions of the secondary components to the total luminosities.

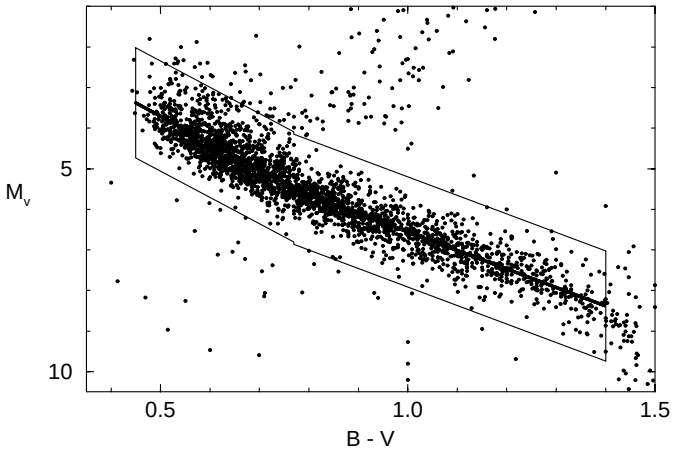

Fig. 1. Selection of the main sequence stars. The F7 to K–type stars with $\pi > 20$ mas and $\delta > -15°$ in the Hipparcos catalogue are plotted in the $((B-V), M_V)$ HR diagram. The thick line is the mean main sequence, and the thin lines marks off the location of the MS stars.

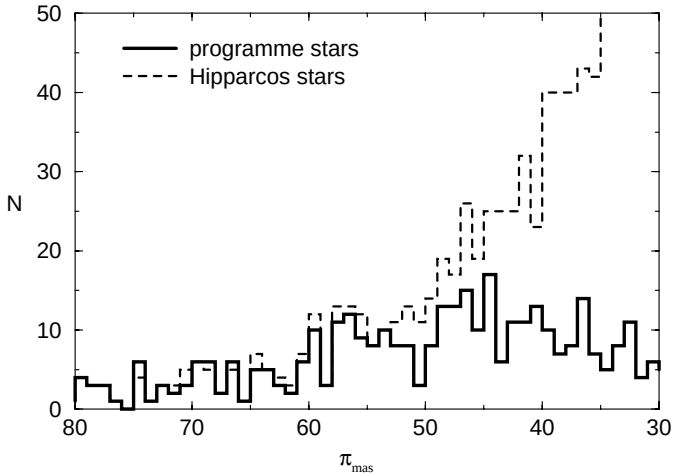

Fig. 2. The distribution of the parallaxes of the MS CORAVEL stars with declinations above $-15°$, as compared to that of the Hipparcos stars.

2.2. The unbiased sample

An important selection effect in studying binarity is the bias toward bright magnitudes (Öpik 1924). This effect acts in favor of binaries with bright secondary components, i.e. with large mass ratios (typically, $q > 0.5$), and it is suspected to be present in the selection of the extended sample. Two origins are possible: first at all, many CNS stars with declinations between -15 and -25 ° were not measured, because they were too faint due to the combination of their magnitudes and of the absorption due to air masses. For this reason, the stars with $\delta < -15°$ are not kept in the *unbiased* sample. This condition lead to the rejection of 21 stars, including 4 SBs. On the other hand, a bias is also suspected in the selection of the sample, since the CNS is far from containing all the nearby stars. The distribution of the parallaxes of the CNS and of the Hipparcos stars selected above is shown in Fig. 2.

The number of Hipparcos stars increases when the parallax decreases. If the selection is complete, the total number of stars

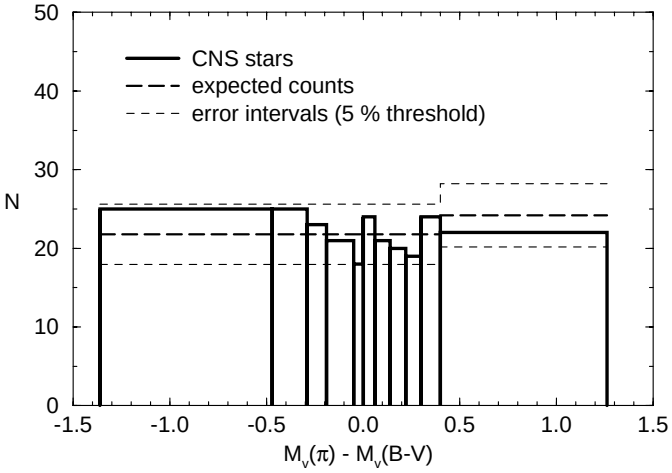

Fig. 3. Distribution of "distances" from MS of the absolute magnitudes of the CNS MS stars with $\delta > -15°$ and $\pi \geq 46$ mas included in the Hipparcos catalogue. The width of the bins is ajusted in order to expect a nearly constant number of stars within each of them. If a bias towards the intrinsically bright stars were present in this part of the CORAVEL sample, the numbers of CNS stars on the left–hand side of the figure should be significantly larger than the expectations derived from Hipparcos stars.

must grow as $1/\pi^3$. It was verified with a Wilcoxon–Mann–Whitney test that this is really what happens, at least for the 570 Hipparcos MS stars with $\pi > 37$ mas: the number of stars with the smallest parallaxes is then even slightly larger than expected. We define thus an unbiased sample of Hipparcos stars, but, unfortunately, the majority of them were not in the CNS when our programme began. These stars were added to the observation runs, but they still have too few measurements to be included in the present study.

The number of CNS stars is almost the same as the number of Hipparcos stars as long as π is larger than 65 mas; some nearby stars are still missing in the CNS, but they are compensated for by the few stars that were not included in Hipparcos. Between 65 and 53 mas, the rate of CNS stars is slightly decreasing, but the difference is still small: only 10 stars, when 189 Hipparcos stars have $\pi > 53$ mas. On the contrary, when the parallaxes are smaller than 53 mas, the rate of CNS stars is clearly decreasing, and it may be suspected that the inclusion of a star in the CNS is then dependent on the magnitude. However, the completeness limit $\pi = 53$ mas would be very drastic, since only 179 stars would be selected, including only 16 SB with known elements and periods shorter than 10 years. Therefore, it was searched if the incompletness of the CNS introduces implicitly a bias in favor of the stars slightly above the MS. This question was tackled by considering the scatter of the CNS stars around the mean MS, as given in Fig. 1. If the CNS stars are distributed in the same way as the Hipparcos stars missing in the CNS, it may be concluded that no bias exists in favour of the binaries with bright secondaries.

The distribution of "distances" from the mean MS is shown in Fig. 3 for the stars with $\pi \geq 46$ mas. A slight excess of luminous stars appears more than 0.2 mag above the main sequence, but it is not significant. In fact, statistical tests show that the CNS stars and the Hipparcos stars that are not in the CNS have distributions very similar: the rejection thresholds of the Wilcoxon–Mann–Whitney test and of the Smirnov test are 97% and 24%, respectively (the rejection threshold is the probability that two sample from the same population look more different than the samples used in the test). It is then assumed that, although the selection of programme stars is not complete up to $\pi = 46$ mas, the sample above this limit is not biased in favor of binaries with large mass ratios. This sample is called the *unbiased* sample hereafter. It contains 240 CNS stars observed with CORAVEL, listed in Table 1.

Table 1. The nearby F7-G-K stars belonging to the unbiased sample according to our new definition. The exponents indicate the spectroscopic binaries with periods shorter than 10 years, as follows: "1" for the SB1, "2" for the SB2, and "3" for a triple system.

GJ	GJ	GJ	GJ	GJ	GJ
5	17.3	23A^3	27	28	30
33	34A	34B	37	41	52
53A	53.1A	56.5	59.1	61	65.1
67	68	69	75	92^2	92.1^1
98AB	105A	106^1	107A	112.1	117
120.2	124	137	141	144	147
153A	155.2	156.2	157A	158	160
160.1AB	161	161.1	166A	171.2A^1	174
183	188A	197	200A	201	202
204	211	217	221	222AB	227
230	231.1A	233A^2	240.1	241	245
249	250A	252	254	257.1	1094
262	273.1	276	282A	290	291A
292.1^1	292.2^1	293.1A	295	302	311
315	324A	325A	327	330.1	334.2
335A	337AB^2	337.1^1	339	340AB	342
348B	349	354.1A	355	356A	365
368	376	379A	380	394	395
396	397	407	414A	417	418
420A	423A^1	423B^1	429A	429B	434
449	451A	454	475	481	483^1
484	486.1	491A^1	502	504	505A
509AB	511.1	2102	517	521.1	527A
528A	538^1	542.2	544A	546	547
549A	556	562	564	566A	566B
567^1	575A	576	579	580AB	583
584A	586A^2	586B	596.1A	598	602
606.2	609.2	611A	614	615.2A^2	615.2B
616	621	626	627AB	631	638
641	649.1A	649.1C	651	653	654.1
659A	659B	672	673	675	678A
684A	688^1	689	702A	704A	706
713AB^2	715	719^2	727	738A	746^1
758	759	762.1^2	762.2	764	765.1A
765.1B	765.4A	767.1B	768.1A	775	775.1
777A	778	779	779.1	783.2A	788
795AB^1	797A	808.2	816.1A	818	819A
820A	820B	824	825.3	836.7	836.8
840	848.4	857.1A	872A	882	886^1
892	894.5	895.4	904	909A^2	914A

Table 2. The nearby F7-G-K stars belonging only to the extended sample. The exponents indicate the spectroscopic binaries with periods shorter than 10 years, as follows: "1" for the SB1, and "2" for the SB2; they are within parenthesis when the RV variability didn't appear in the Coravel measurements.

GJ	GJ	GJ	GJ	GJ	GJ
6	16.1	25*A*	31.4	34.1[2]	39
42.1	44	50	53.2	54.2*B*	55.2
56	56.3*A*	56.4	57.1*A*	57.1*B*	58.2[2]
59.2	1040	71	74	82.1	83.2
87.1*A*[2]	90	91.1*A*	91.2*A*	99.1	105.6[2]
112	113	114	118.2*A*	120.1*A*	120.1*C*[1]
121.2	128*A*	135	138.1*A*[1]	142	147.1
1063	150.2	1064*A*	1064*B*[1]	1069[1]	165.1
165.2	168	171[1]	173.1*A*[1]	176.2	177
177.1	2035	182.1	189.1	198	1076
209	214	223	224	226.2	226.3
256	267	282*B*	285.1[1]	295.1	296.2[2]
297.2*A*	301.1	307.1	310.1*A*[1]	310.1*B*	313
1113	321	334.1	338.1*A*	340.2	340.3
1124[2]	341.1	343.1[2]	378.1	387*A*	388.2[1]
389.1	392*A*	398.1	402.1	1139	421.1*B*
423.1	426*A*	433.2*A*	433.2*B*[1]	435.1	439
441[2]	444*A*	452.3*A*	452.3*B*	458.1*AB*	464.1
469.1[1]	469.2*A*	1160[2]	479.1	488.2	489[1]
496*A*	498	500[1]	503.2	506	506.2
511	518.2*A*	521.2*A*	1176	523	529
541.1	554[(1)]	559.1	561	563.3	569.1
570*A*	573	577	1189	579.3	1190
580.2	1192	591	593*AB*	610[2]	612
615.1*A*	615.1*B*	629.2*A*[1]	632	632.1	632.2*A*
634.1	637.1	639	640	650[1]	658
663*A*	663*B*	664	679	692.1[1]	694.1*B*
697	698	700.2	702.2	703	708.4
718	722.1	725.1	743	747.2	753
754.2	1237[2]	761*A*	761.1	764.1*A*	764.1*B*
764.2	765.2	765.3	773.2	773.3[2]	781.2
783.1*AB*	789	791.3	792.1*AB*	793.1[1]	1255*AB*[(2)]
794.3	1255*D*	1259[1]	814	823	828.4
838.1*A*	838.2	838.3*A*	850	851.4[2]	854
862.1[1]	867.1*A*	870[1]	1272*AB*	871.2	878.1*A*
893.2*B*	894.4	904.1*A*	907.1	908.1	909.1

2.3. The sample of SB in the solar neighbouhood

The extended sample contains 61 spectroscopic systems with periods up to 10 years, including a triple one and two SB which escaped detection with CORAVEL: the radial velocity of GJ 554 was constant in Coravel observations, but the star was detected as SB with the Elodie spectrograph, and it could have been detected with Coravel; it is provisionally kept in the sample, until the study of the selection effects. The other undetected SB is GJ 1255 A, which is a W UMa–type binary with broad spectral lines due to rotation. This will not be taken into account in the derivation of the properties of unevolved systems, since its mass ratio and its period were modified by mass exchange. One obtains then an extended sample of 61 spectroscopic orbits. Among them, 27 orbits are also in the unbiased sample. This number looks small when compared to the 23 orbits of G-type stars used by Mazeh et al. (1992). The reason is that only 10 of these orbits are still in the unbiased sample, since 9 were shifted to the extended sample and 4 were discarded because the stars are not on the main sequence. Meanwhile, we added one G-type star with a period longer than the 3000 days limit that they applied, and 16 late–type stars.

Table 3. The SB1 with $P < 10$ years and with unknown mass ratios in the extended sample of solar neighbourhood stars: Elements used in the derivation of the distributions of the mass ratios and of the periods. The flag "*x*" designates the stars which don't belong to the unbiased sample but to the extended sample. The "*a*" exponent after the mass function indicates when the astrometric orbits were also taken into account, as explained in Sect. 6.1.2. The sources of the spectroscopic elements are coded as follows: (1) Paper II, (2) Paper IV, (4) Jasniewicz & Mayor (1988), (5) Abt & Levy (1976), (6) van de Bos (1928), (7) Berman (1931).

GJ	P	e	K_1	$f_{\mathcal{M}}$	$\mathcal{M}_1$	$\epsilon_{\rm RV}$	ref
	days		km s^{-1}	$\mathcal{M}_\odot$	$\mathcal{M}_\odot$	km s^{-1}	
23 A	2.1	0.00	48.98	0.01844	1.19	1.342	1
92.1	80.0	0.33	14.49	0.0212	0.77	0.323	2
138.1A^x	321.6	0.50	7.47	0.0090	1.05	0.334	1
1064 B^x	48.6	0.66	10.05	0.00216	0.75	0.374	2
171.2A	1.8	0.00	10.45	0.000212	0.75	0.343	2
310.1A^x	14.3	0.33	21.95	0.0132	1.19	0.362	1
337.1	16.2	0.09	35.3	0.0733	1.12	0.348	5
388.2^x	298.3	0.94	4.81	0.000139^a	1.03	0.374	2
423 A	669.2	0.53	8.0	0.0214	1.05	0.528	6
423 B	4.0	0.00	5.0	0.000052	1.05	0.664	7
469.1^x	25.9	0.22	8.08	0.0013	0.87	0.348	4
500^x	20.5	0.56	7.94	0.000612	0.89	0.346	1
692.1^x	2558.4	0.94	9.06	0.00862^a	0.79	0.335	2
746	22.0	0.08	13.42	0.00546	0.92	0.305	1
795 A	918.6	0.69	3.36	0.00139	0.67	0.350	2
870^x	374.6	0.44	8.03	0.0146^a	0.56	0.386	2

The extended and unbiased samples contain 34 and 17 SB1, respectively. However, thanks to the astrometric orbital elements derived in Paper IV, the mass ratios are fixed with errors smaller than 0.05 for 18 and 9 of them, respectively. These stars are listed with the SB2 in Table 4. The remaining 16 SB1, including three with inaccurate astrometric orbital elements, are listed in Table 3. The mean errors of the radial velocity measurements, $\epsilon_{\rm RV}$, are included since the selection effects depend on them. For these stars, the mass ratios are unknown, but probability distributions of q may be derived from the mass functions, as explained in Sect. 6.1.

The numbers of SB2 in the extended sample and the unbiased sample are 27 and 10, respectively. These stars are listed in Table 4. Notice that the SB2 frequency is smaller amongst the unbiased sample than amongst the extension to the extended sample: $10/27 = 37\%$, in place of $17/34 = 50\%$; this confirms the efficiency of the selection effect in favour of luminous secondaries in the extended sample.

3. The spectroscopic binaries in open clusters

3.1. The open cluster surveys

At the same time as the SB surveys in the solar neighbourhood, two open clusters were observed with CORAVEL: the Pleiades

Table 4. Same as Table 3, but for the SB with known mass ratios. The SB1 with mass ratios derived from the astrometric orbits are indicated by the index "1" in the q column. For the SB2, ϵ_{RV} is the average error of the RV measurements of the primary component, as obtained from the reduction process. It must be divided by 1.4 in order to correct for the contamination by the secondary component, as explained in Sect. 5.3. The sources of the spectroscopic elements are coded as follows: (1) Paper II, (2) Paper IV, (3) Duquennoy & Mayor (1988).

GJ	P days	e	K_1 km s^{-1}	q	$\mathcal{M}_1$ $\mathcal{M}_\odot$	ϵ_{RV} km s^{-1}	ref
23 AB	2527.0	0.77	10.90	0.66	1.7	1.342	1
34.1^x	13.8	0.24	57.31	0.96	1.19	0.724	1
58.2^x	11.0	0.04	38.87	0.84	0.75	0.365	2
87.1A^x	94.8	0.69	19.08	0.97	1.19	0.548	1
92	10.0	0.00	10.49	0.88	1.05	0.485	3
105.6^x	330.9	0.66	21.03	0.92	1.12	0.518	1
106	1227.2	0.49	6.48	0.42^1	0.67	0.331	2
120.1C^x	554.6	0.56	1.30	0.22^1	0.75	0.326	2
1069^x	716.1	0.09	1.32	0.36^1	0.67	0.393	2
171^x	330.4	0.65	7.91	0.29^1	0.75	0.322	2
173.1A^x	610.0	0.40	4.55	0.23^1	0.73	0.374	2
233 A	7.0	0.15	56.99	0.84	0.79	0.285	2
285.1^x	551.9	0.39	9.87	0.58^1	1.05	0.330	2
292.1	161.1	0.28	5.69	0.19^1	0.75	0.339	2
292.2	447.3	0.36	5.85	0.32^1	0.85	0.395	1
296.2^x	243.8	0.42	18.16	0.93	1.19	0.615	2
337 AB	987.9	0.42	11.52	0.99	0.82	0.482	2
1124^x	3.8	0.00	71.18	1.00	0.75	0.545	2
343.1^x	8.5	0.10	56.45	0.99	0.56	0.688	2
433.2B^x	23.5	0.41	24.31	0.48	0.75	0.370	1
441^x	632.6	0.25	10.05	0.94	0.56	0.507	2
1160^x	1284.4	0.50	9.78	0.86	0.75	0.465	2
483	271.7	0.88	1.47	0.21^1	0.73	0.302	2
489^x	3571.3	0.77	2.48	0.18^1	0.70	0.359	2
491 A	103.2	0.15	1.66	0.25^1	0.79	0.344	2
538	3607.4	0.52	6.78	0.60^1	0.85	0.322	1
554^x	2636.8	0.71	0.90	0.05^1	0.73	0.336	2
567	125.4	0.51	19.0	0.57^1	0.75	0.294	2
586 A	889.8	0.98	37.33	0.68	0.75	0.313	2
610^x	105.9	0.15	23.55	0.88	0.72	0.430	2
615.2A	1.1	0.00	63.01	0.99	1.19	2.094	1
629.2A^x	133.1	0.27	16.11	0.57	0.92	0.543	1
650^x	386.7	0.42	6.14	0.42^1	0.99	0.361	3
688	83.7	0.20	5.68	0.50^1	0.73	0.302	2
713 AB	280.9	0.44	18.06	0.70	1.26	0.521	2
719	6.0	0.30	28.43	0.89	0.58	0.444	2
1237^x	166.8	0.14	13.95	0.90	0.73	0.475	2
762.1	494.7	0.34	9.43	0.95	0.77	0.505	2
773.3^x	1770.9	0.50	4.78	0.85	1.19	0.497	2
793.1^x	57.3	0.31	28.73	0.80	0.82	0.406	1
1259^x	2173.3	0.46	1.93	0.14^1	0.73	0.332	2
851.4^x	650.3	0.60	15.70	0.76	0.79	0.534	2
862.1^x	632.5	0.41	11.26	0.58	1.26	0.375	2
886	454.7	0.52	2.45	0.23^1	0.70	0.309	2
909 A	7.8	0.00	46.74	0.95	0.73	0.443	2

and Praesepe. The spectral types covered by the cluster surveys range from mid–F to early–K, and are therefore slightly earlier than in the solar neighbourhood sample.

The MS stars of the Pleiades were observed over 8 years, from 1978 to 1986. Eighty–eight stars brighter than B = 12.5 mag received four or five RV measurements, and half of the sample still got an additional observation in 1990–1991. A few stars fainter than B = 12.5 were also observed, but the frequency of the measurements was lower, since they were added in the course of the programme, and since they required the best sky conditions. The SB received more observations as soon as they were detected, and the orbital elements of 11 of them, including 2 SB2, were finally obtained (Mermilliod et al. 1992). The periods are all shorter than 10 years.

The Praesepe MS stars were observed from 1978 to 1996. Seventy–nine stars brighter than B = 12.5 mag were observed four to nine times. One star must still be added, although it was not observed at all: the radial velocity of the W Uma–type eclipsing binary KW 244 = TX Cnc cannot be measured with CORAVEL, since its rotational velocity is too fast. This star will be taken into account in the binary frequency, but not in the derivation of other statistical properties, since its mass ratio was probably modified by mass exchange since the formation of the binary. Again, some stars fainter than B = 12.5 were also observed, but less frequently than the others. The binaries get additional observations and the orbital elements were finally derived for 18 cluster stars, including a triple system completely solved (KW 367) and 2 SB with periods longer than 10 years. Therefore, 17 orbits with $P < 10$ years were obtained, 13 SB1 and 4 SB2 (Mermilliod et al. 1994; Mermilliod & Mayor 1999).

3.2. The extended and the unbiased samples of open cluster SB

Merging the two clusters, one obtains a sample of 28 spectroscopic orbits, 22 SB1 and 6 SB2. However, as for the nearby stars, we must address the question of the completeness of the sample and of the existence of a possible bias in favour of large mass ratios. Stars with primary components fainter than B = 12.5 were less observed than the others, except when the contribution of the secondary to the total luminosity made the magnitude of the system brighter than this limit. Therefore, only the SB with primary magnitudes brighter than B = 12.5 are kept in the *unbiased sample* hereafter. 25 orbits are thus selected. The 3 remaining ones (2 SB1 and 1 SB2) belong to the *extended sample* however, and they will be taken into account to derive the distribution of mass ratio until q = 0.5.

Unlike the nearby SB, the orbits of the cluster SB1 cannot be completed by astrometric data coming from Hipparcos. However, important constraints on the mass ratios were derived from the positions of the systems relative to the photometric main sequence of the cluster. Maximum secondary masses were thus obtained, and they were included in the original publications. The mass ratios of 7 SB1 of the unbiased sample were even completely fixed by this method. There were only constraints for 15 additional SB1 which are listed in Table 5; no constraint was obtained from photometry for the long period component orbiting KW 367, but the maximum mass ratio was derived assuming that its mass is less than that of the primary

Table 5. Same as Table 3, but for the SB1 of the Pleiades and of Praesepe.

name	P	e	K_1	$f_{\mathcal{M}}$	$\mathcal{M}_1$	q_{Max}	$\epsilon_{\rm RV}$
	days		km s^{-1}	$\mathcal{M}_\odot$	$\mathcal{M}_\odot$		km s^{-1}
HII 522^x	23.8	0.10	4.85	0.00028	0.85	0.64	0.51
HII 571	15.9	0.33	26.46	0.0258	0.93	0.59	0.47
HII 2172	30.2	0.33	15.20	0.0093	1.05	0.53	0.56
HII 2406	33.0	0.52	25.95	0.037	0.95	0.59	0.53
HII 2407^x	7.1	0.00	19.67	0.0056	0.82	0.44	0.52
HII 3097	774.0	0.78	5.09	0.0027	0.98	0.57	0.65
KW 47	34.6	0.41	19.01	0.0189	1.22	0.48	0.65
KW 127	13.3	0.23	17.82	0.0072	1.07	0.37	0.45
KW 268	144.3	0.65	13.25	0.0153	1.23	0.47	0.68
KW 365	51.2	0.66	23.4	0.028	1.02	0.70	0.66
KW 367	1659.0	0.76	8.32	0.0269	1.90	0.55	0.64
KW 416	25.8	0.43	26.94	0.03850	1.31	0.45	0.46
KW 434	3.9	0.00	33.27	0.01504	0.97	0.36	0.50
KW 439	457.8	0.17	2.62	0.00082	1.34	0.45	0.57
KW 508	647.6	0.50	4.72	0.0046	1.08	0.23	0.52

Table 6. Same as Table 4, but for the SB of the Pleiades and of Praesepe with fixed mass ratios. The correction to apply to $\epsilon_{\rm RV}$ is the same as in Table 4, but it concerns all SB with $q > 0.7$. The exponent "1" in the q column indicates the SB1 with mass ratio derived from photometry.

name	P	e	K_1	q	$\mathcal{M}_1$	$\epsilon_{\rm RV}$
	days		km s^{-1}		$\mathcal{M}_\odot$	km s^{-1}
HII 173	479.7	0.10	15.79	0.95	0.90	0.63
HII 320	757.1	0.31	11.0	0.81[1]	0.92	0.59
HII 761	3.3	0.00	51.33	0.65[1]	1.02	0.56
HII 1117	26.0	0.57	13.4	0.93	1.00	0.65
HII 2027	48.6	0.30	17.37	0.94[1]	0.90	0.95
KW 142	46.0	0.22	32.50	0.99	1.19	1.38
KW 181	5.9	0.36	47.13	0.61[1]	1.12	0.60
KW 184^x	47.4	0.34	23.46	0.99	0.83	0.61
KW 325	896.9	0.12	8.79	0.66[1]	1.09	0.53
KW 367	3.1	0.00	52.88	0.83	1.04	0.64
KW 368	76.6	0.21	14.53	0.35[1]	0.95	0.45
KW 495	35.9	0.19	38.3	0.93	1.15	0.88
KW 540	1149.5	0.67	4.05	0.65[1]	1.02	0.47

of the close pair. The mean errors of the radial velocity measurements of the Pleiades stars were taken from Mermilliod et al. (1992). Those of the Praesepe stars were not included in the original publication, but they were communicated by J.-C. Mermilliod.

The 6 SB2 and the 7 SB1 with fixed mass ratios are presented together in Table 6.

4. The complete SB samples

We want to consider together the SB of the solar neighbourhood and that of the open clusters, but we need to be sure that the binaries in these two places are statistically similar.

4.1. Comparing the nearby and cluster SB: The mass ratios

We notice that the unbiased sample of cluster SB contains 6 SB2 amongst 25 orbits. This is rather few when compared to the rate obtained from the nearby SB: 10/27. However, the difference comes from the difficulty in detecting the secondary peak for the cluster stars, which are faint and therefore very close to the observation limit of CORAVEL, unlike the nearby stars. This was confirmed by a comparison of the distributions of the mass ratio functions of each sample, defined as

$$Y = f_{\mathcal{M}}/\mathcal{M}_1 = \frac{q^3}{(1+q)^2}\sin^3 i \qquad (1)$$

where $f_{\mathcal{M}}$ is the mass function and i the inclination of the orbit. Y was derived for the SB2 as for the SB1, and it appeared that the cluster SB have in fact values of Y, and therefore of q, slightly larger than the nearby ones. However, the difference is not statistically significant, since the Smirnov test indicates that the rejection threshold of the hypothesis that the samples are both equivalent is as large as 29% (the rejection threshold is the probability of finding discrepancies even larger in comparing two samples randomly extracted from the same population). It could also come from the selection effects, since the cluster stars received less measurements and have larger RV errors than the nearby stars. It is then assumed hereafter that the cluster SB obey the same mass ratio distribution as the nearby ones. Nevertheless, the hypothesis that the cluster SB intrinsically obeys the same mass ratio distribution as the nearby SB will still be re-considered in Sect. 7.1.3.

4.2. Comparing the nearby and cluster SB: The periods and eccentricities

The distribution of periods of cluster SB stars was compared to that of nearby SB. It seems that the frequency of long periods is smaller for cluster SB than for the nearby SB, but the difference is not significant, since the distributions are similar at the 23% threshold of significance. Again, the discrepancy could also be due to the difference in selection effects between the two samples.

Finally, we considered the eccentricities of the orbits. Since this parameter is correlated with the period, all the SB were plotted on a period–eccentricity diagram (Fig. 4). It was thus verified that all samples are distributed within the same limits in $\log P$ and e.

4.3. Merging the nearby and cluster SB

Adding the SB of the solar neighbourhood and that of the open clusters, an extended sample of 89 orbits is finally obtained. The unbiased sample contains 52 orbits. The total number of SB2 is 36, but, thanks to the help of the astrometric elements or of the photometric deviations, the mass ratios are finally fixed for 58 SB of the extended sample, and 31 SB of the unbiased sample. Only 15 SB1 in the extended sample, or 9 in the unbiased sample, have mass ratios constrained only by their mass functions.

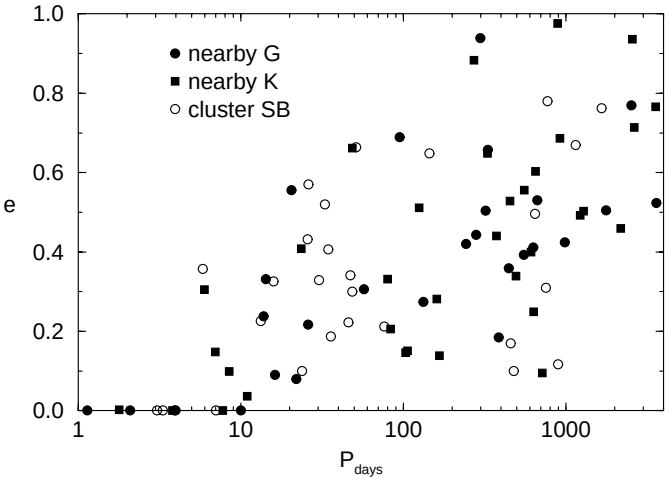

Fig. 4. Distribution of the SB of the extended samples in the period–eccentricity diagram.

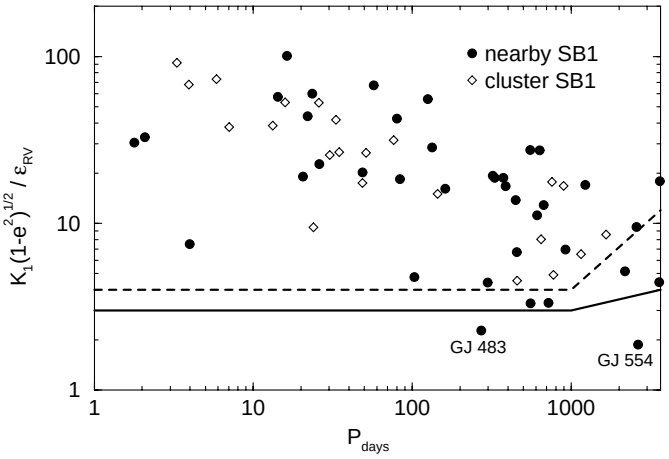

Fig. 5. Derivation conditions of the orbital elements of the discovered SB1. It is assumed that the spectroscopic orbits of the SB1 discovered in the solar neighbourhood were derived only when $K_1 \sqrt{1-e^2}/\epsilon_{RV}$ is above the plain line; the orbits of GJ 483 and GJ 554 were obtained from ELODIE measurements. In the open cluster sample, the completeness limit is in dashes.

5. Selection effects: conditions for recording a SB orbit

The SB surveys among nearby stars and in the open clusters were both planned in two steps: the detection of the SB, and the derivation of the orbits. In the present section, the conditions for missing a SB orbit are searched, in order to take them into account in the derivation of the intrinsic statistical properties of binaries in Sect. 6.2.

5.1. SB detection

First of all, the stars received a few measurements over a few years, and the SB were selected when the scatters of their RV were so large that $P(\chi^2)$ was less than 1%. In practice, many SB were already selected in the course of the detection survey, since they exhibited large RV variations, and they were observed more often; it is assumed, however, that this facility didn't change the fact that these stars would all have $P(\chi^2) < 1\%$ at the end of the survey, even if they had not been selected before. The effect of this detection method was investigated in Paper II (see their Fig. 4). It appeared that the probability law of the SB detection is not simple, but that it depends on the distribution of the epochs of the measurements. For this reason, the efficiency of the detection process will be evaluated by simulations, taking into account the time–table of the detection survey.

5.2. Derivation of the orbital elements of the SB1

Despite our efforts, it was not possible to derive the orbits of all the SB that were detected in the survey. The majority of the stars left aside are long–period binaries (including some visual binaries), but a few may be short–period binaries with small RV amplitudes. In order to investigate this question, we considered the SB1 with known orbits; the semi–amplitudes of RV of the primary components, K_1, were expressed in relation to the mean RV errors, ϵ_{RV}. Moreover, we paid attention to the fact that a large eccentricity does not facilitate the derivation of the orbit, although it makes K_1 larger than for a circular orbit. Therefore, we considered the value that K_1 would have if the eccentricity were null, that is $K_1 \sqrt{1-e^2}$, and we determined the ability to derive a spectroscopic orbit as a function of this parameter.

The SB1 of the extended sample are all plotted in a (P, $K_1 \sqrt{1-e^2}/\epsilon_{RV}$) diagram, as shown in Fig. 5. It appears that the derivation of the orbits is more complete in the solar neighbourhood than in the clusters. This is a consequence of the survey duration, and of the effort dedicated to the search for brown dwarf companions 10 years ago. Some SB1 with small radial velocity variations detected with CORAVEL were even observed with the ELODIE spectrograph on the 1.93 meter telescope at the Haute-Provence Observatory, and their orbital elements were thus obtained even when $K_1 \sqrt{1-e^2}$ is very small. Therefore, two SB1 are below the completeness limit drawn in Fig. 5: about 50 CORAVEL measurements only provided an approximative orbit of GJ 483, and 20 ELODIE measurements were also used to derive the final elements; this star lies at the limit of the CORAVEL capabilities, and it would be hazardous to assume that the orbital elements of any detected SB having similar (P, $K_1 \sqrt{1-e^2}/\epsilon_{RV}$) were certainly derived; the other is GJ 554, which was even not variable in the CORAVEL measurements. Since a couple of SB1 found with CORAVEL in Paper IV were not observed with ELODIE and didn't get an orbit, these SB will be discarded for homogeneity, when the statistics will be corrected for selection effects in Sect. 6.2.

5.3. The transition between SB1 and SB2 orbits

Since the SB2 are binaries with luminous, and therefore massive, secondary components, it should be possible to assign a maximum mass ratio for the SB1. This limit will be used in deriving the probability distribution of the mass ratio of each SB1, in Sect. 6.1. Since it is impossible to distinguish the secondary

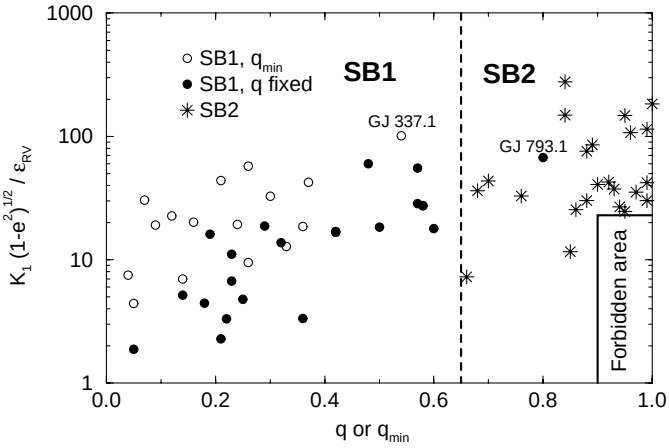

Fig. 6. The transition between SB1 and SB2 for the nearby stars. It is infered from this figure that the SB1 were not classified as SB2 because their mass ratios are less than 0.65. Moreover, the SB with $q > 0.9$ and $K_1\sqrt{1-e^2} > 23\epsilon_{RV}$, if any, did not get orbital solution although they may have been detected as "line width spectroscopic binaries" (LWSB).

peak when it is near to the primary, it is expected that the transition from SB1 to SB2 could depend not only on q, but also on $K_1\sqrt{1-e^2}/\epsilon_{RV}$. Therefore, the SB1 of the extended sample of solar neighbourhood stars are plotted on a (q, $K_1\sqrt{1-e^2}/\epsilon_{RV}$) diagram, in Fig. 6 (GJ 433.2B and GJ 793.1 are plotted on this figure as SB1, since their secondary components were not detected on the CORAVEL measurements). The cluster SB are not represented, since a simple look at Table 5 is sufficient to see that their photometric limits on q are already rather small when compared to the actual q of the SB1 in Table 6.

Before adding the SB2 to the (q , $K_1\sqrt{1-e^2}/\epsilon_{RV}$) diagram, we must be sure that ϵ_{RV} is the same as if the primary component were alone. In reality, it appears that ϵ_{RV} is on average 1.4 larger for the SB2 than for the SB1. This is certainly due to the contamination of the correlation peak of the primary component from that of the secondary. We tried to relate this excess in ϵ_{RV} to q and to the maximum RV difference, $K_1 + K_2$, but the scatter of ϵ_{RV} is rather large and no obvious relation was found. Therefore, for the SB2, the values of ϵ_{RV} as they are given in Table 4 are systematically divided by 1.4 hereafter (a similar correction was found in the open cluster sample, but for all SB with $q > 0.7$). After this correction, the SB2 are plotted on Fig. 6. They all have $q > 0.65$, whereas only one SB1 lies beyond this limit: GJ 793.1, which was detected as SB2 according to Mazeh et al. (1997). It is rather surprising that the limit in mass ratio does not seem related to $K_1\sqrt{1-e^2}$. However, this point is not important in practice, because the only SB1 with unfixed q that is relatively close to the limit is GJ 337.1, which has also the largest $K_1\sqrt{1-e^2}/\epsilon_{RV}$.

An interesting feature in Fig. 6 is the lack of SB2 with $q > 0.9$ and $K_1\sqrt{1-e^2}$ smaller than 23 ϵ_{RV}. We interpret it as the effect of a bias against the detection of SB2 with twin components, since the correlation peaks are merged in a single symmetric blended peak when the RV amplitude is small. Such binaries may be detected as "line width spectroscopic binaries" (LWSB), but the derivation of their orbital elements is rather hazardous. Therefore, in correcting for selection effects, it will be assumed that these systems were not resolved in our survey.

6. Statistical properties of binaries: Method

Before deriving the intrinsic distributions of mass ratios, we derive the distribution of mass ratios of the sample of observed stars. The mass ratios of the SB2 and of several SB1 were directly obtained, but the remaining SB1 deserve a dedicated treatment.

6.1. Distribution of q for a sample of SB1

6.1.1. When only the mass ratio function is available

The minimum information about the mass ratio of a SB1 lies in the mass ratio function (Eq. (1)). We don't know the inclination i, but we assume that it obeys a $\sin i$ distribution, corresponding to random orientations of the orbital planes. Boffin et al. (1992) and Mazeh & Goldberg (1992) were the first to apply the Richardson–Lucy algorithm to the derivation of the distribution of mass ratios, f_q from a set of values of Y. The basic principle is to assume a preliminary distribution for f_q (i.e. a constant distribution) at the beginning of the iterative process, and to calculate, for each SB1, the probability distribution of its actual mass ratio. Mazeh & Goldberg did this calculation using the partial derivative of Y with regard to q. In practice, the calculation is easier when the partial derivative of Y is taken with regard to i. The probability distribution of q for a SB1 with the mass ratio function Y is then:

$$\varphi_q(q) = f_q(q)\ \sin i_Y(q)\ \tan i_Y(q)\ /\ C_{\rm Norm} \qquad (2)$$

where $i_Y(q)$ is the inclination corresponding to the value q that is considered and to the value of Y actually observed. $C_{\rm Norm}$ is a constant that is adjusted in order to fit the condition :

$$\int \varphi_q(q)\mathrm{d}q = 1. \qquad (3)$$

As Mazeh & Goldberg, we assigned a maximum value to the mass ratios of the SB1, which corresponds to the visibility limit of the secondary spectrum as derived in Sect. 5.3, or which is the limit for photometry, as indicated in Table 5. The histogram of the probability of q is thus derived for each SB1, and it is added to the histogram of q for all the SB of the sample. A new estimation of f_q is finally obtained by connecting the centers of the bins of this histogram, and it is used in the next iteration until convergence.

6.1.2. Contribution to f_q of SB1 with astrometric orbits

This section concerns only three SB1 in Table 3: GJ 388.2, GJ 692.1 and GJ 870. The semi–major axis of the astrometric orbit of GJ 388.2, as derived in Halbwachs et al. (2000), is very small: $a_0 = (1.39 \pm 0.41)$ mas, and the orbit is not significant in fact (Pourbaix & Arenou 2001). It should then not be taken into account, a priori. However, if the mass ratio of this binary were equal to the maximum for a SB1, the actual semi–major

axis would be $a_1(q = 0.65) = 11.8$ mas, and the astrometric orbit would then obviously be significant. Therefore, neglecting the non–existence of a significant orbit for this star would introduce a bias in our statistic. We decide then to take a_0 and σ_{a_0} into account, using the same error model as in Halbwachs et al. (2000). The two other stars have significant astrometric orbits in Paper IV, but with errors too large to directly derive q. They deserve the same treatment as GJ 388.2: The calculation of $\varphi_q(q)$ above is slightly modified, and Eq. (2) becomes:

$$\varphi_q(q) = \frac{f_q(q)\ \sin i_Y(q)\ \tan i_Y(q)\ f_{a_0}(a_0 \mid a_1(q), \sigma_{a_0})}{C_{\rm Norm}} \qquad (4)$$

where $f_{a_0}(a_0 \mid a_1(q), \sigma_{a_0})$ is the frequency distribution of the observed semi–major axis a_0, when the actual value is $a_1(q)$ and when the error is σ_{a_0}; $a_1(q)$ depends on $i_Y(q)$, on the orbital element $a_1 \sin i$, and on the trigonometric parallax, π :

$$a_1(q) = \frac{\pi\ a_1 \sin i}{\sin i_Y(q)}. \qquad (5)$$

We derive $\varphi_q(q)$ from Eq. (4) assuming that f_{a_0} obeys a Rayleigh–Rice distribution.

It would also be possible to take into account the astrometric orbits of some other stars of Table 3, for which non significant astrometric orbits were derived. However, the error model based on the Rayleigh–Rice distribution is only an approximation, and its use must be restricted to small samples, when the random noise coming from the counts is larger than the error coming from the model. For this reason, we want to take the astrometric orbits into account only when they lead to important constraints on the mass ratios. We derived the maximum semi–major axes $a_1(q = 0.65)$ that could have all the SB1 in Table 3. Apart from the 3 exceptions above, and apart from a few stars for which the Hipparcos measurements are non–existent or unusable, none is larger than the smallest a_0 found for the significant astrometric orbits in Paper IV, which is 3.7 mas. Therefore, taking these additional astrometric orbits into account could introduce biases instead of improving our results. We prefer to ignore them.

6.2. Correction of the selection effects

We use a correction method in its principle similar to that of Mazeh & Goldberg (1992). Due to selection effects, the distributions of mass ratios, but also of periods, which were obtained directly from the sample do not refer to binaries in space. Correcting these distributions is an iterative process, since the correction of the distribution of P depends on the actual distribution of q, and vice versa.

Let's start with a derivation step of the distribution of P. For each SB of the sample, we search $D(P)$, the proportion of binaries with the same period as the SB and for which the orbital elements were derived. $D(P)$ was computed by simulations, generating virtual observations of virtual binaries with various orbital inclinations and various mass ratios, and counting the virtual binaries fulfilling the conditions seen in Sect. 5. Finally, the sample SB received the weight $1/D(P)$ and it was added to the histogram of the periods.

The correction of the distribution of q is based on the same principle. For each value of q, the proportion of binaries selected in our sample, $D(q)$, is calculated. Now, the virtual binaries have various orbital orientations, various periods, but also various eccentricities; we use the expression of the distribution of eccentricities by Künzli & North (1998), in order to take into account the relation between e and P. When the mass ratio of a SB is not known, this calculation is done in the course of the derivation of φ_q explained just above in Sect. 6.1.

The intrinsic distributions of P and q are thus derived, but also an evaluation of the number of binaries which escaped selection. The errors are derived by Jackknife computation. The distribution of mass ratios up to $q = 0.5$ is derived from the extended sample, but only the unbiased sample is used to derive f_q for $q > 0.5$. The results are presented in the next section.

7. Statistical properties of binaries: Results

7.1. Distribution of mass ratios

7.1.1. The whole sample: F7-G dwarfs with $P < 10$ yr

The distribution of the mass ratios of all the SB with periods less than 10 years is plotted in Fig. 7a.

Three main features appear in this distribution. From right to left, the first one is a peak around $q = 1$. This peak is not an artefact coming from an excessive correction of the bias against SB2 twin components, since it is already visible in the distribution of mass ratios of some 15 SB of the unbiased sample with $q \geq 0.7$. In order to verify that it is not due to random variations in the count, we considered the null hypothesis "f_q is constant for $q \in [0.7\ ,\ 1]$" in a Kolmogorov–Smirnov test that was applied on the unbiased sample, without correction for incompleteness. The rejection was only 3%, and, since the selection effects play against the detection of twins (cf the end of Sect. 5.3), this indicates that this feature is probably real. It will be investigated in Sect. 7.1.4 whether this peak comes from wide binaries as well as from the close ones.

A second peak appears around $q = 0.65$. This is also the maximum value of q that is permitted for a SB1 in the sample of nearby field stars, and it may be suspected that the peak was an artefact generated by the computation method. However, it was verified that it remains at the same place when the transition between SB1 and SB2 is shifted toward large values of q. Therefore, the minimum at $q = 0.75$ which is well marked in panels (a) to (c) is probably real. It was suggested that the peak around $q = 0.65$ could be generated by evolved binaries, where the initial primary components were turned in white dwarfs whereas the initial secondary components are the present primaries. This explanation doesn't look very satisfactory, because the peak should then be wider than in Fig. 7, since the primary masses are in a large range. Its shape would then have been largely altered by random noise.

A third and last peak is found around $q = 0.25$. Alternatively, it may be assumed that the minimum between this peak and the previous one is entirely a product of random noise in the small sample that we consider, and that the second peak ranges in reality from $q = 0.1$ to $q = 0.7$. Whatever

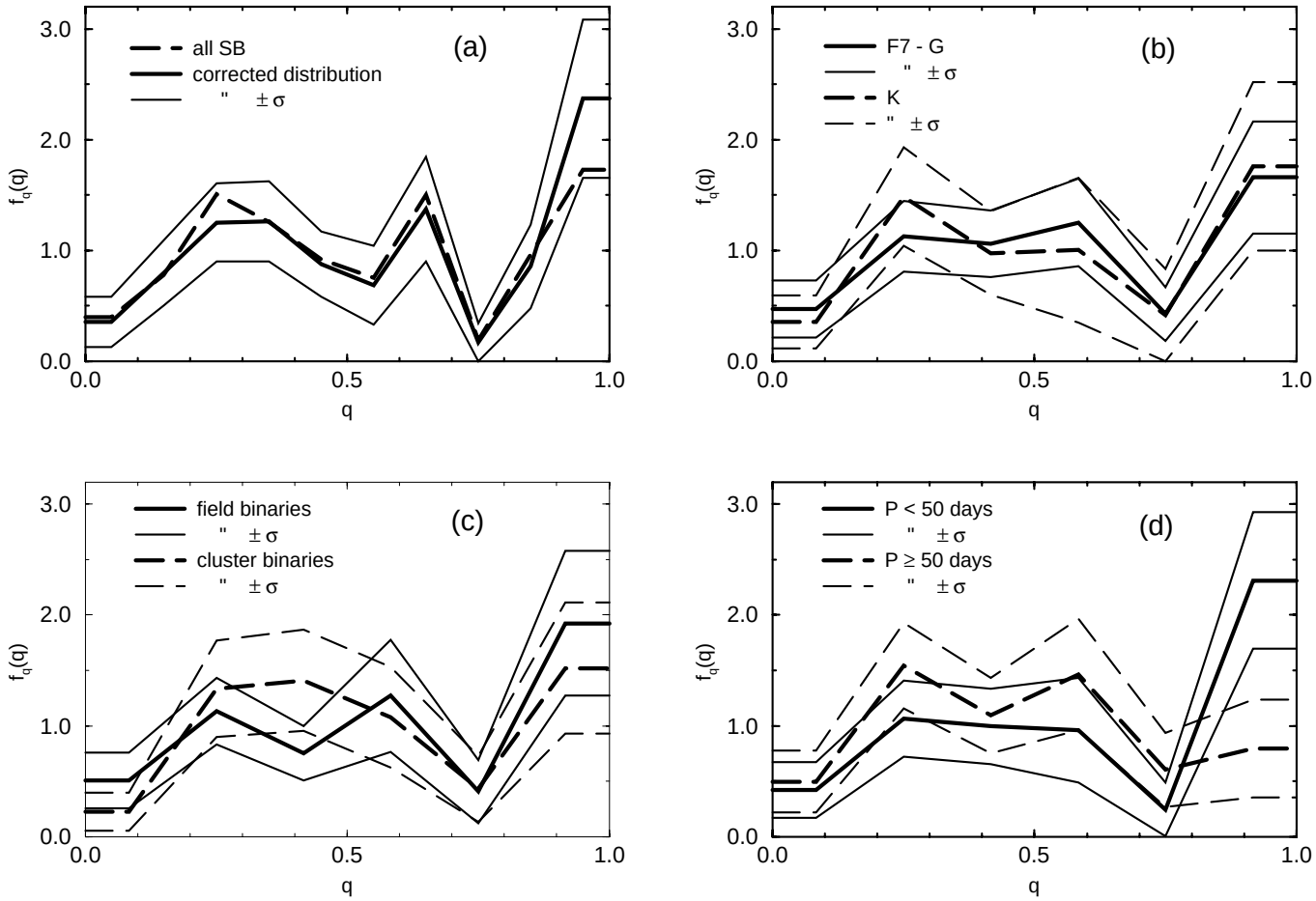

Fig. 7. Distribution of the mass ratios. As in the calculations, the distributions are drawn by joining the centers of the bins; the mass ratios range is divided in 10 equal bins in panel (a), and in 6 bins in the others. **a)** derived from the nearby SB and from the cluster SB with $P < 10$ years; the observed distribution refers to all the SB, without any restriction about the ability to derive their orbital elements with CORAVEL; **b)** the F7–G stars compared to the K-type stars; **c)** the binaries in open clusters compared to the binaries in the solar neighbourhood; **d)** the short–period binaries compared to the long–period binaries.

the number of peaks, the distribution is decreasing on the left side, when small mass ratios are considered. The low frequency that we found for small mass ratios even concerns companions beyond the hydrogen–ignition limit: assuming a period of 100 days, which is nearly the median of the sample, and the median inclination $i = 60$ deg, a one solar mass binary with q as small as 0.03 would have $K_1 \sqrt{1-e^2} = 1.2$ km s^{-1}, which corresponds roughly to the limit for deriving the orbit. Therefore, we find again the *brown dwarf desert* that was found with a larger sample of brown dwarf candidates (Halbwachs et al. 2000). In that context, take note of the decrease of the distribution of masses for the giant planets from 2 to 10 Jupiter masses, delimiting the low mass side of the desert of brown dwarfs (Jorissen et al. 2001).

7.1.2. Does f_q depend on the spectral type?

We implicitely assume that the formation process of stars is *scale free*, generating binaries obeying a certain mass ratio distribution. However, the formation of the secondary components could depend on the mass of the primary, and the distribution of $\mathcal{M}_2$ could be related to $\mathcal{M}_1$ – apart from the fact that $\mathcal{M}_2 \leq \mathcal{M}_1$. Therefore, the distribution of mass ratios would depend on the primary mass.

The sample was split in two parts, according to the primary spectral types, and the intrinsic distributions of q were derived again. The results are in Fig. 7b. Apart from minor differences easily explained by random variations, the distributions look very similar; each one is always within the 1 σ interval of the other one. More surprisingly, the three peaks present in the overall distribution are present again. Nevertheless, the intermediate peak cannot be attributed to white dwarf components for the K-type SB, since the mass ratio should then be around 1. However, it is now rather flat, and it may appear simply by chance.

7.1.3. Is f_q the same for cluster binaries as for field binaries?

We had already checked on the raw data that the cluster SB obey the same distribution of mass ratios as the SB in the solar neighbourhood (Sect. 4.1). In order to compare the corrected distributions, they were derived for the two samples and they

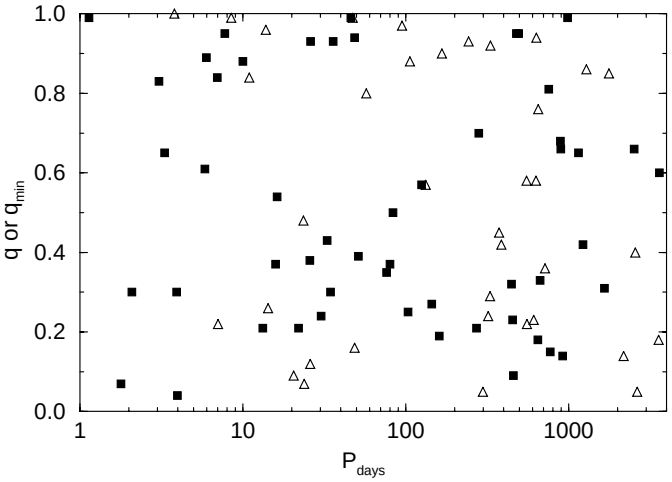

Fig. 8. The period–mass ratio diagram of the binaries of the extended sample. The filled squares refer to the SB belonging to the unbiased sample, and the triangles to the SB only in the extended sample. The mass ratios of some SB with $q < 0.65$ are not determined, and the lower limits are then assumed.

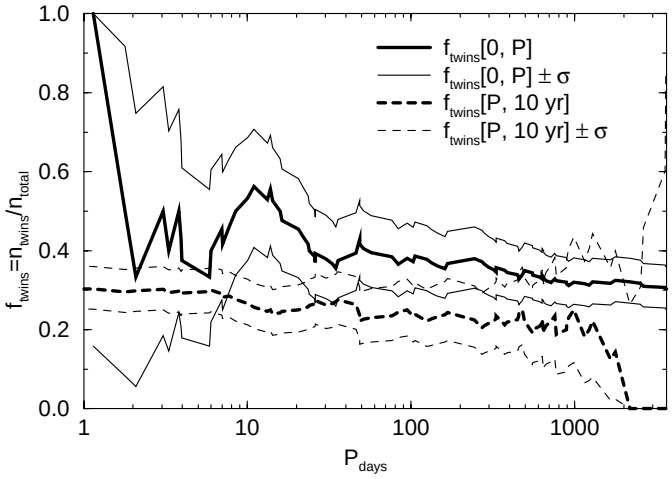

Fig. 9. The frequency of twins among the SB of the extended sample, as a function of the limit in period. The full line is the frequency of $q > 0.8$ among SB with periods shorter than P in abscissa, when the dashed line is the same but for periods longer than P.

are plotted in Fig. 7c. A single look is sufficient to be convinced that they seem identical.

7.1.4. Does f_q depend on the period?

It is well established that the distribution of mass ratios derived from the visual binaries with wide separations doesn't contain a peak around $q = 1$ (see for instance Halbwachs 1983). Therefore, since the peak of the twins seems to be real, a transition between these two regimes necessarily exists. According to Tokovinin, the frequency of twins should fall off for P longer than 40 days. In order to verify this limit, all the 89 SB of the extended sample were plotted on a period–mass ratio diagram, Fig. 8. Since the unbiased sample contains two SB with large mass ratios and periods between 40 and 50 days, it seems that 50 days would be more appropriate than 40.

We have also derived the frequency of twins as a function of the limit in period. Figure 9 gives the proportions of binaries with $q > 0.8$ among the SB with periods shorter than P (full line), and also among the SB with periods longer than P (dashed line). Notice that the curves never cross, confirming that, whatever the limiting period, the frequency of twins is always larger among the short period binaries than among the others. The curves with thin lines are the limits of the true frequencies compatible with the observed ones, assuming the threshold 15.87% (which corresponds to one standard deviation for the normal distribution). The noise due to the small counts is so large that the twin frequency among the short periods is well separated from the frequency among the long periods only around two values of P: the first one is between 10 and 20 days, where is a large hump in the twin frequency among the short period SB; the second one is near $P = 50$ days, which definitely seems the best candidate limit for discriminating the SB with a large proportion of twins and those with only a few twins. Nevertheless, this limit comes from the noise in the counts and from the definition of the sample, but not from the nature of binary stars; it is used hereafter to emphasize the relation between f_q and P, but it is clear from Fig. 9 that the rate of twins is gradually decreasing from $P = 10$ days to $P = 10$ years, and still probably beyond this limit, in agreement with Söderhjelm (1997).

The distributions of mass ratios derived from the SB with $P < 50$ d and from the others are presented in Fig. 7d. The frequency highly rises for $q > 0.8$ in the short period group, while it is low for the long periods. The discrepancy is also quite visible before correcting for the selection effects: in the raw counts, the unbiased sample contains 24 short period SB, amongst which 10 with $q > 0.8$. For comparison, it contains also 28 long period SB, but with only 4 with $q > 0.8$; the probability to get a so small frequency only by chance, as derived from the hypergeometric distribution, is only 3%. However, since the scarcity of twins is increased by the selection effects, the significance of the test is not so drastic. If the selection effects were as important for the short periods as for the long periods, we should count 22 short period SB (in place of 24), including 8 with $q > 0.8$ (in place of 10). The rates to be compared become then 4 twins among 28 long period SB, and 8 twins among 22 SB with $P < 50$ d. The probability to obtain the observed discrepancy would then be about 7%. Therefore, we cannot definitely exclude that the distribution of mass ratios doesn't depend on the period, although our result suggests that the peak of twins could be due to a process generating preferably equal mass binaries with periods below 50 days.

7.2. Distribution of periods

The histogram of the periods of the SB of the extended sample is shown in Fig. 10. The selection effects were corrected as explained in Sect. 6.2, assuming two distributions of mass ratios, both derived from the extended sample: the former was obtained from the SB with $P < 50$ d, and the latter from the others. The results are shown in Fig. 10. The distribution of $\log P$ is clearly rising until about 10 days. It would be tempting

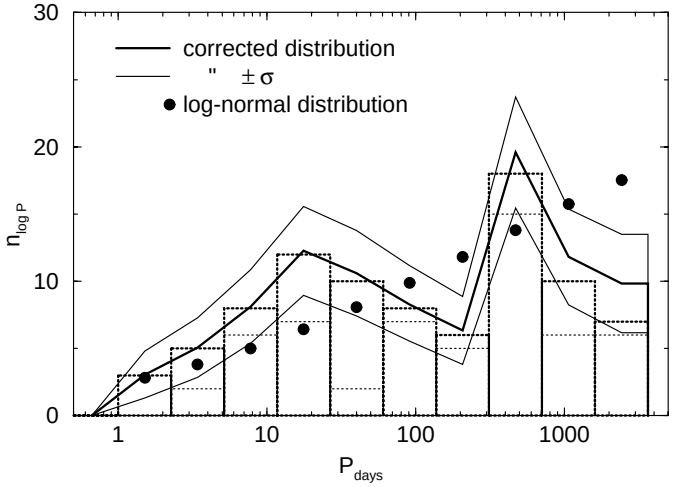

Fig. 10. Distribution of the periods of binaries. The histogram in thick dots refers to the SB of the extended sample, and the thin dots represent the contribution of nearby stars. The distribution corrected for selection effects is in solid line. The big dots represent the log–normal distribution found in Paper II.

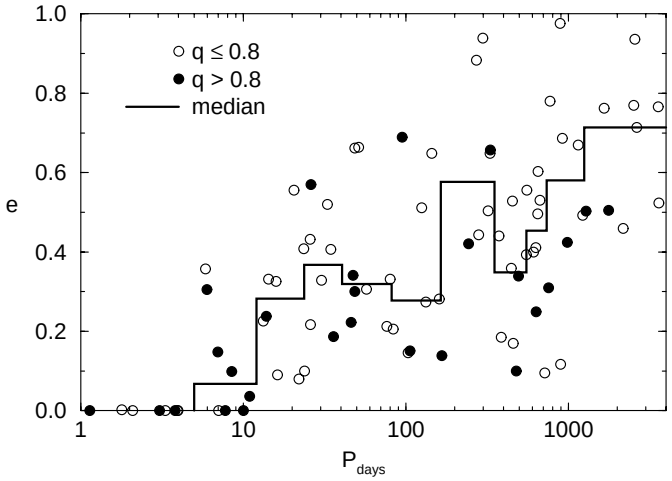

Fig. 11. Same as Fig. 4, but discriminating the mass ratios larger than 0.8 from the others. Apart from the last bin, the median eccentricity is indicated for bins of 8 SB.

to relate the broad peak centered at about 20 days to the excess of twins, but, although this interpretation looks possible, it is rather hazardous since the peak could as well be produced by random variation in the counts. The sharp peak between 1 and 2 years is much more marked, but no more significant: a χ^2-test at the 10% level shows that, in reality, the uncorrected distribution may be constant for the 7 last bins of the observed histogram, i.e. from about 12 days to 10 years.

The Gaussian distribution of $\log P$ derived in Paper II is also plotted in Fig. 10 for comparison. It was used to derive the distribution that should follow the observed SB, and a χ^2–test was used to check whether it is compatible with the histogram of the real sample. The agreement is rather bad: when the extended sample is considered, the rejection threshold of the Paper II distribution is a bit less than 5%. However, the counts fit well when the cluster sample is discarded. In Paper II already, it was pointed out that the Hyades SB don't obey the log–normal period distribution. Therefore, although the distribution of periods of both samples is not significantly different, it is possible that, in reality, cluster SB have periods shorter than field SB. Alternatively, the parameters of the distribution could be revised, or the distribution of periods could even be more complex than the log–normal law. This question will be tackled in Paper V, when the distribution of periods will be derived on the full range of that parameter (Eggenberger et al., in preparation).

7.3. Eccentricities

Since twins seem to be generated by a process other than binaries with unequal components, it was searched to see if they have different eccentricities. In order to take into account the correlation between eccentricities and periods, we consider the positions of twins in the period–eccentricity diagram (Fig. 11). It appears that, among the SB with the same period, the SB with $q > 0.8$ have on average eccentricities smaller than the others.

We performed a statistical test in order to verify if this discrepancy is significant. For periods longer than 5 days, the diagram was divided in bins of 8 SB (or a bit more for the last bin), having nearly the same period, and the median eccentricity was derived. The twins in the lower part of the diagram were counted, and we calculated the probability to get this number assuming a random distribution. It was derived from the hypergeometric distribution that the probability to obtain so many twins or even more is 1.35%, leading to the rejection of the random hypothesis at the level 2.7%. The test was repeated using only the SB of the unbiased sample, and also discarding the first bin (i.e. $P < 12$ d). Although the numbers of SB were then smaller, the test is not less significant: the rejection thresholds are 1.6 and 1.3% respectively. We wondered whether this discrepancy could be due to a selection effect, but this explanation was ruled out: on the one hand, a large eccentricity slightly decreases the scatter of the radial velocity, making the detection a bit more difficult, but, on the other hand, the semi–amplitude of radial velocity increases, and it is easier to derive the orbit. Moreover, this is not true only for twins, but for all SB. We conclude then that the orbits of twins are really less eccentric than that of the other SB having the same period. It is worth noticing that this feature is not restricted to the period shorter than the limit of 50 days, but it concerns the whole period range above the circularization period, or, at least, above about 12 days.

7.4. The rate of binary and multiple stars

7.4.1. Multiplicity versus spectral type in the solar neighbourhood

We investigate now a possible correlation between binarity and the spectral types of the stars. In order to tackle this problem, we use the unbiased sample of nearby stars, which covers the range of spectral types from F7 to late K (whereas the cluster sample is restricted to the earlier of these types). In practice, the colour indices $B - V$ are more adequate for statistical tests

than the spectral types, for which only a few discrete values are permitted. Therefore, the 240 stars of the sample were sorted according to $B-V$, and the ranks of the 26 systems with periods less than 10 years were put in a Wilcoxon–Mann–Whitney test. It was found that the rate of binary and multiple systems doesn't seem to depend on $B-V$, since the probability of obtaining random variations as large as those obtained was larger than 50%. Since the detection is close to complete for this sample (see Sect. 7.4.2 hereafter), we conclude that the proportion of close binaries is constant from late–type F stars until late–type K stars.

7.4.2. The binary frequency in the solar neighbourhood

We counted 26 systems with $P < 10$ years in the unbiased sample of nearby stars, including one triple system, and one star below the completeness condition. This leads to a raw frequency of $10.8^{+2.2}_{-1.9}\%$ (the error intervals of frequencies correspond to 1 rms hereafter). The minimum mass ratio is 0.04.

When the selection effects are taken into account, the unbiased sample contains only 25 systems above the completeness limit, but it is estimated that 1.9 systems escaped detection. Therefore, the frequency of stars having at least one companion with $q > 0.04$ and $P < 10$ yr is $26.9/240 = 11.2^{+2.2}_{-1.9}\%$.

7.4.3. Comparison to the multiplicity in open clusters

We have seen in Sect. 3 that 28 systems, including a triple one and a W UMa eclipsing binary, were found among 168 stars brighter than 12.5 mag. Three SB were discarded since their primary components were fainter than this limit, and we finally obtained an unbiased sample of 165 stars containing 25 systems with periods less than 10 years. The raw rate is $25/165 = 15.1^{+3.0}_{-2.6}\%$. Our calculation lead to an estimation of 2.9 undetected systems, and the corrected rate is then $16.9^{+3.1}_{-2.7}\%$. This looks larger than the rate found above for the nearby stars, but the discrepancy is not significant at the 10% level.

When we merged the unbiased samples of nearby stars and of cluster stars, we get the corrected multiplicity rate: $13.5^{+1.8}_{-1.6}\%$.

7.4.4. Do twins prefer multiple systems?

It was suggested (Tokovinin 2000) that short–period SB2 with large mass ratios could preferably appear in multiple systems. A simple look at Table 4 is sufficient to see that some twins are A–components of visual systems, but we must verify if the rate of such multiple systems is really abnormally large. Since no twin was found among components apart from primaries, we consider hereafter the $H0$ hypothesis: "primary components are more frequent among twins than among other stars". If this hypothesis is significantly ruled out hereafter, it will be worthwhile to look also at the rate of visual components but otherwise not, since the significance of the test would then be worse.

The unbiased sample of nearby stars seems to be more appropriate to tackle this question, since the discovery of wide systems is then more complete: we count 62 A–components among the 240 stars in Table 1, but only 37 among the 216 stars of the extension in Table 2. The unbiased sample contains 5 nearby SB with $q > 0.8$ and $P < 50$ d, and 3 of them are primary components of wide binary or multiple systems. According to the hypergeometric law, the probability to get 3 A–components or even more among 5 stars randomly selected in the unbiased sample is 11%. This probability is too large to exclude that the large frequency of primary components among close twins was found by chance.

Notice that taking the long–period twins does not ameliorate the significance of the excess of A–components : three A–components are now counted among 7 twins, and the probability to get a so large rate by chance is then 26%. We compared also the frequency of A–components among twins (3/7) to the frequency of A–components among all the SB of the unbiased sample (9/27), but the probability to get this excess by chance is 43%. Therefore, although we found more primary visual components among the twins than among the other stars, we cannot consider that this excess is significant.

7.4.5. False alarms and true exoplanets

It was suspected that a large proportion of exoplanets discovered by the radial velocity technique could be brown dwarfs or even low mass stars in reality (Han et al. 2001). These false alarms were assumed to be generated by low inclinations of the orbital planes. Since exoplanets are usually searched for around bright G-type dwarfs, we derived the number of false alarms expected among the G-type stars of the unbiased sample: assuming the average distribution of mass ratio in Fig. 7a, the frequency of SB looking like planet candidates is 0.34%. Therefore, assuming the rate of binary systems found above, we obtained 0.05 SB looking like exoplanet candidates among 102 bright G-type stars. In reality, candidate planets were found around 8 stars: GJ 61=υ And (Butler et al. 1997), GJ 324 = 55 Cnc (Butler et al. 1997), GJ 407 = 47 UMa (Butler & Marcy 1996), GJ 527A = τ Bootis (Butler et al. 1997), GJ 606.2 = ρ CrB (Noyes et al. 1997), GJ 765.1B = 16 Cyg B (Cochran et al. 1997), GJ 848.4 = HD 210277 (Marcy et al. 1999), and GJ 882 = 51 Peg (Mayor & Queloz 1995). The astrometric wobble of ρ CrB looks too large for a planetary component, and the system could be a pole–on binary (Gatewood et al. 2001; Pourbaix & Arenou 2001), although Zucker & Mazeh (2001) pointed out that the significance of this wobble is not really convincing when the number of planet candidates which were examined is taken into account. Nevertheless, even considering ρ CrB as a binary star, we count one false alarm among the 8 candidate planets, when 0.05 false alarms are expected on average. The probability to get one false alarm was then about 5%, and the occurence of this one, which is more questionable, is not really alarming. The rate of stars actually harbouring planets, as derived from the present data, is then at least $7/102 = 6.9^{+3.6}_{-1.8}\%$, and it will certainly increase when the planets with low masses and long periods will be accessible.

8. Conclusion

8.1. Summary and discussion

We used the results of two large and intensive radial–velocity surveys to investigate the distributions of mass ratios and of periods of binary stars with dwarf primary components from F7 to late K types. We obtained results free of selection effects for binaries with secondaries in a range of masses covering all the stellar masses and overlapping with the brown dwarfs, and with periods as long as 10 years.

No difference was found between the field binaries and the cluster binaries, considering the distributions of mass ratios, of periods and eccentricities, or the binary frequency. This result is in agreement with Kähler (1999), and with the references cited therein.

The distribution of mass ratios is the same for the whole range of spectral types, i.e. from F7 to the late K stars. This invariance indicates that the binary formation is scale free when $P < 10$ yr, unlike the predictions of the dynamical model of non–hierarchical $N > 2$–fragmentation (see Clarke 2001; Bate et al. 2002b). Nevertheless, the distribution of mass ratios that we obtained seems in agreement with the results of the simulation of Bate et al., since they finally obtained 7 binaries distributed in two twins ($q > 0.9$) and five binaries with mass ratios between 0.3 and 0.7.

The distribution of mass ratios depends on the period, since short period binaries include more systems with mass ratios of 0.8 or more (twins). An important difference discriminating the twins from binaries with unequal components is the eccentricity of their orbits, which is significantly lower when the period is longer than 10 days. This feature concerns the periods at least of 10 years, indicating that the efficiency of the peculiar twin formation process is not restricted to the short periods. This statistical correlation would be a touchstone for the model used by Bate et al. (2002b), but, unfortunately, they didn't pay attention to the eccentricities in the presentation of their results. Considering the formation processes summarised in Sect. 1.1, this suggests that twins were generated by accretion of a gaseous envelope with a large specific angular momentum. However, since this process leads an increase of the separation, it must be combined with interactions with a circumbinary disk in order to obtain periods as small as a few days. The later evolution of the disk could results in the formation of additional components with wide separations, although our statistics are too poor to investigate this hypothesis.

Apart from the twins, the distribution of mass ratios of close binaries is not different from that of binaries with long periods. Both exhibit a broad or a double peak from $q = 0.2$ to about $q = 0.7$. The large eccentricites of these systems suggests that they were formed at wide separations, but their components moved closer by interaction with circumbinary disks. The scarcity of binaries with mass ratios below $q = 0.2$, i.e. with secondary masses lighter than about 0.15 $\mathcal{M}_\odot$, is probably due to accretion from the disk.

The distribution of $\log P$ is rather flat from about 10 days until 10 years, and the existence of a peak corresponding to twins and/or migration toward the close separations seems quite possible. Unfortunately the errors due to small counts are rather large, and this hypothesis needs to be confirmed in the future. The global behaviour of the distribution of periods on the full range of that parameter will be discussed in Paper V (Eggenberger et al., in preparation).

The frequency of binary and multiple systems with periods shorter than 10 years is $13.5^{+1.8}_{-1.6}$%. The frequency doesn't depend of the spectral type of the primaries and it is very close to the 14% of SB expected among T Tau stars (Guenther et al. 2001), confirming that the rate of binaries among disk stars is not age–dependent.

The proportion of binaries with stellar components that appear as stars harbouring planets is only about 0.3%. Since the frequency of stars with planets is about half of the frequency of binaries, the rate of false alarms is almost negligible. The high frequency of planets, separated from the binary stars by the "brown dwarf desert" in the mass ratio distribution, firmly supports the hypothesis that these two kinds of objects are generated by different processes.

8.2. Future prospects

The present study was restricted to the SB, and therefore to periods shorter than 10 years. It will be extended soon to the visual binaries and the wide pairs, as was done in Paper II.

Although we used the largest unbiased sample ever considered, our results are still affected by large uncertainties coming from statistical noise. When the observations of the Hipparcos supplement to the unbiased sample will be completed, about 30 SB orbits will be added and the transition between short period and long period binaries could become more visible in the statistic. Improvements are still expected when the large surveys dedicated to the search for planetary systems will be fully completed. High precision RV measurements are now regularly obtained for more than two thousand solar–type stars (Udry et al. 2001), and a sample of SB four or five times larger than the one that we obtained should be available within a few years.

Acknowledgements. Dr J.-C. Mermilliod kindly supplied us with the mean errors of the Coravel radial velocity measurements of the Praesepe SB. We are grateful to Dr Tsevi Mazeh for the discussion we had when he presented his iterative algorithm. We thank the anonymous referee for helpful suggestions, and for relevant comments about the formation models. We acknowledge the continuous support provided by the Swiss Research Foundation. This paper has made use of the Simbad database maintained by the CDS in Strasbourg, and of the Extrasolar Planets Encyclopaedia of Jean Schneider.

References

Abt, H. A., & Levy, S. G. 1976, ApJS, 30, 273
Artymowicz, P. 1983, Acta Astron., 33, 224
Artymowicz, P., & Lubow, S. H. 2001, in The Formation of Binary Stars, ed. H. Zinnecker, & R. D. Mathieu, IAU Symp., 200, 439
Artymowicz, P., & Lubow, S. H. 1994, ApJ, 421, 651
Artymowicz, P., Clarke, C. J., Lubow, S. H., & Pringle, J. E. 1991, ApJ, 370, L35
Bate, M. R. 2000, MNRAS, 314, 33
Bate, M. R. 2001, in The Formation of Binary Stars, ed. H. Zinnecker, & R. D. Mathieu, IAU Symp., 200, 429

Bate, M. R., Bonnell, I. A., & Bromm, V. 2002a, MNRAS, 332, L65
Bate, M. R., Bonnell, I. A., & Bromm, V. 2002b, MNRAS, in press
Berman, L. 1931, Lick Obs. Bul., 15, 109
Bodenheimer, P., & Burkert, A. 2001, in The Formation of Binary Stars, ed. H. Zinnecker, & R. D. Mathieu, IAU Symp., 200, 13
Boffin, H. M. J., Paulus, G., & Cerf, N. 1992, in Binaries as Tracers of Stellar Evolution, ed. A. Duquennoy, & M. Mayor (Cambridge Univ. Press), 26
Bonnell, I. 2001a, in École CNRS de Goutelas 2000, Étoiles doubles: Des étoiles à grandes séparations aux binaires X, ed. D. Egret, J.-L. Halbwachs, & J.-M. Hameury (Observatoire de Strasbourg), 307
Bonnell, I. 2001b, in The Formation of Binary Stars, ed. H. Zinnecker, & R. D. Mathieu, IAU Symp., 200, 23
Bonnell, I., & Bate, M. R. 1994, MNRAS, 271, 999
Branch, D. 1976, ApJ, 210, 392
Butler, R. P., & Marcy, G. W. 1996, ApJ, 464, L153
Butler, R. P., Marcy, G. W., Williams, E., Hauser, H., & Shirts, P. 1997, ApJ, 474, L115
Clarke, C. J. 2001, in The Formation of Binary Stars, ed. H. Zinnecker, & R. D. Mathieu, IAU Symp., 200, 346
Cochran, W. D., Hatzes, A. P., Butler, R. P., & Marcy, G. W. 1997, ApJ, 483, 457
Duquennoy, A., & Mayor, M. 1988, A&A, 200, 135
Duquennoy, A., & Mayor, M. 1991, A&A, 248, 485
Duquennoy, A., Mayor, M., & Halbwachs, J. L. 1991, A&AS, 88, 281
ESA 1997, The Hipparcos Catalogue, ESA SP-1200
Gatewood, G., Han, I., & Black, D. 2001, ApJ, 548, L61
Gliese, W. 1969, Veröff. Astron. Rechen Inst. Heidelberg, No 22
Gliese, W., & Jahreiss, H. 1979, A&AS, 38, 423
Gliese, W., & Jahreiss, H. 1991, Catalogue of Nearby Stars, 3rd Edn., preliminary version
Guenther, E. W., Joergens, V., Neuhaüser, R., et al. 2001, in The Formation of Binary Stars, ed. H. Zinnecker, & R. D. Mathieu, IAU Symp., 200, 165
Günther, R., & Kley, W. 2002, A&A, 387, 550
Halbwachs, J. L. 1981, Thèse de 3e cycle, Observatoire de Strasbourg
Halbwachs, J. L. 1983, A&A, 128, 399
Halbwachs, J. L. 1987, A&A, 183, 234
Halbwachs, J. L., Arenou, F., Mayor, M., Udry, S., & Queloz, D. 2000, A&A, 355, 581
Han, I., Black, D. C., & Gatewood, G. 2001, ApJ, 548, L57
Heacox, W. D. 1995, AJ, 109, 2670
Heacox, W. D. 1998, AJ, 115, 325
Jasniewicz, G., & Mayor, M. 1988, A&A, 203, 329
Jorissen, A., Mayor, M., & Udry, S. 2001, A&A, 379, 992
Kähler, H. 1999, A&A, 346, 67
Künzli, M., & North, P. 1998, A&AS, 127, 277
Lucy, L. B., & Ricco, E. 1979, AJ, 84, 401
Marcy, G. W., Butler, R. P., Vogt, S. V., Fischer, D., & Liu, M. C. 1999, ApJ, 520, 239
Mathieu, R. D. 2001, in The Formation of Binary Stars, ed. H. Zinnecker, & R. D. Mathieu, IAU Symp., 200, 593
Mayor, M., & Queloz, D. 1995, Nature, 378, 355
Mazeh, T., & Goldberg, D. 1992, in Binaries as Tracers of Stellar Evolution, ed. A. Duquennoy, & M. Mayor (Cambridge Univ. Press), 170
Mazeh, T., Goldberg, D., Duquennoy, A., & Mayor, M. 1992, ApJ, 401, 265
Mazeh, T., Martin, E. L., Goldberg, D., & Smith, H. A. 1997, MNRAS, 284, 341
Mermilliod, J. C., Rosvick, J. M., Duquennoy, A., & Mayor, M. 1992, A&A, 265, 513
Mermilliod, J. C., Duquennoy, A., & Mayor, M. 1994, A&A, 283, 515
Mermilliod, J. C., & Mayor, M. 1999, A&A, 352, 479
Morbey, C. L., & Griffin, R. F. 1987, ApJ, 317, 343
Noyes, R. W., Jha, S., Korzennik, S. G., Krockenberger, M., & Nisenson, P. 1997, ApJ, 483, L111
Öpik, E. J. 1924, Pub. Obs. Astron. Univ. Tartu XXV, No 6
Pourbaix, D., & Arenou, F. 2001, A&A, 372, 935
Söderhjelm, S. 1997, in Visual Double Stars: Formation, Dynamics and Evolutionnary Tracks, ed. J. A. Docobo, A. Elipe, & H. McAlister (Astrophysics and Space Science Library, Kluwer), vol. 223, 497
Staniucha, M. 1979, Acta Astron., 29, 587
Stepinski, T. F., & Black, D. C. 2000, A&A, 356, 903
Tokovinin, A. A. 2000, A&A, 360, 997
Tout, C. A. 1991, MNRAS, 250, 701
Trimble, V. 1974, AJ, 79, 967
Trimble, V. 1978, Observatory, 98, 163
Udry, S., Mayor, M., Arenou, F., & Halbwachs, J. L. 2002, A&A
Udry, S., Mayor, M., & Queloz, D. 2001, in Planetary Systems in the Universe: Observation, Formation and Evolution, ed. A. Penny, P. Artymowicz, A.-M. Lagrange, & S. Russel, ASP Conf. Ser., IAU Symp., 202, in press
van den Bos, W. H. 1928, Mem. Acad. R. Sc. Let. Denmark 8th Ser., 12, 295
Zucker, S., & Mazeh, T. 2001, ApJ, 562, 549